*Journal of Integrative Agriculture 2026, 25(8): 3240–3253*

Available online at ScienceDirect

KeAi CHINESE ROOTS GLOBAL IMPACT

**Journal of Integrative Agriculture**



RESEARCH ARTICLE

# Root-specific upregulation of the $Na^+/K^+$ transport genes mitigates salt stress in blueberry

**Huifang Song[1*], Bingshuai Du[1*], Xinyan Zhao[1], Kaiyue Feng[1], Lingyun Zhang[1, 2#], Yibo Cao[1, 2#]**

[1] *State Key Laboratory of Efficient Production of Forest Resources/Key Laboratory of Forest Silviculture and Conservation of the Ministry of Education/ College of Forestry, Beijing Forestry University, Beijing 100083, China*

[2] *Research & Development Center of Blueberry, Beijing Forestry University, Beijing 100083, China*

**Highlights**

- Ion transport pathways were enriched under salt stress, and root-upregulated $Na^+/K^+$ transport genes promoted blueberry salt tolerance.
- Leaf $Na^+$ and $K^+$ contents strongly correlated with *VcHAK5*, *VcNHX1*, and *VcNHX2* expression.
- Knockdown of *VcHAK5*, *VcNHX1*, and *VcNHX2* increased salt sensitivity in blueberry calli.
- Reciprocal grafting showed that root $Na^+/K^+$ homeostasis is critical for salt tolerance.

**Abstract**

Soil salinization is a growing challenge for highbush blueberry (*Vaccinium corymbosum*) production, but knowledge about its physiological and molecular responses to salt stress remains limited. To address this, we performed Gene Ontology (GO) enrichment analysis and weighted gene co-expression network analysis (WGCNA) on differentially expressed genes from the roots and leaves of the salt-tolerant cultivar 'Duke' and the salt-sensitive cultivar 'Sweetheart'. GO analysis revealed significant enrichment of ion transport and cellular ion homeostasis in the roots under salt stress. WGCNA identified a strong correlation between $Na^+$ and $K^+$ contents and the expression of hub genes *VcHAK5*, *VcNHX1*, and *VcNHX2* under salt stress. These genes were significantly upregulated in the roots of the salt-tolerant cultivar. *VcHAK5* encodes a $K^+$-selective ion transporter in the plasma membrane, and *VcNHX1* and *VcNHX2* encode $Na^+/H^+$ and $K^+/H^+$ antiporters in the tonoplast. Knockdown mutants of these genes in blueberry calli showed hypersensitivity to salt stress. Furthermore, reciprocal grafting between salt-sensitive and salt-tolerant blueberry cultivars demonstrated that lower root $Na^+$ content and $Na^+/K^+$ ratios are crucial for salt tolerance. This study provides the first comprehensive insights into blueberry responses to salt stress, identifies target genes and highlights the critical role of salt-resistant roots.

**Keywords:** blueberry, soil salinization, salt tolerance, ion transport, grafting

## 1. Introduction

Soil salinization is a critical abiotic stressor that greatly restricts crop growth and production globally (Munns and Tester 2008; Zhu 2016; Zhao *et al.* 2020). Sodium ($Na^+$) is the primary soluble cation; it enters the plant root and is delivered to the shoot. Excessive $Na^+$ accumulation in shoots leads to ion toxicity, disrupts metabolism, and reduces productivity (Munns and Tester 2008; Ishikawa and Shabala 2019). To cope with high salt conditions, plants have evolved various salt tolerance mechanisms to mitigate the toxic effects of $Na^+$. These include reducing $Na^+$ uptake, enhancing $Na^+$ exclusion and sequestration, and maintaining intracellular $Na^+/K^+$ homeostasis (Munns and Tester 2008; Wang *et al.* 2020; van Zelm *et al.* 2020), with ion transporters playing an important regulatory role.

High-affinity potassium transporters (HKTs), a class of

Received 27 March 2025; Received in revised form 14 August 2025; Accepted 25 September 2025; Available online 5 December 2025
Huifang Song, E-mail: songhuifang1010@bjfu.edu.cn; #Correspondence Yibo Cao, E-mail: caoyibo@bjfu.edu.cn; Lingyun Zhang, Tel: +86-10-62336044, E-mail: lyzhang@bjfu.edu.cn

*These authors contributed equally to this study.

© 2026 CAAS. Publishing services by Elsevier B.V. on behalf of KeAi Communications Co. Ltd. This is an open access article under the CC BY-NC-ND license (http://creativecommons.org/licenses/by-nc-nd/4.0/). Peer review under responsibility of Editorial Board of *Journal of Integrative Agriculture*.
doi: 10.1016/j.jia.2025.12.004

plasma membrane-localized proteins, have been found to decrease sodium ($Na^+$) transport from roots to leaves and alleviate $Na^+$ toxicity. Wheat TaHKT2;1, *Arabidopsis* AtHKT1, rice SKC1 (shoot $K^+$ content), durum wheat Nax1/2 ($Na^+$ exclusion 1/2), maize ZmHKT1;1, ZmHKT1;2, ZmHAK4, cultivated tomato SlHAK20, soybean GmHKT1, grapevine VviHKT1;1, and blueberry VcHKT1;1, and all of these play a critical role in mediating $Na^+$ transport and influencing $Na^+$ distribution between roots and shoots (Schachtman and Schroeder 1994; Rubio *et al.* 1995; Ren *et al.* 2005; Munns *et al.* 2012; Chen *et al.* 2014; Deinlein *et al.* 2014; Henderson *et al.* 2018; Zhang *et al.* 2018, 2019, 2023; Huang *et al.* 2020; Wang *et al.* 2020; van Zelm *et al.* 2020; Song *et al.* 2023). Plant vacuolar $Na^+/H^+$ antiporters (NHXs) facilitate electroneutral $Na^+/H^+$ exchange by sequestering excessive $Na^+$ from the cytosol into vacuoles (Blumwald and Poole 1985; Apse *et al.* 1999; Gaxiola *et al.* 1999). Based on subcellular localization, NHXs were consistent with three main functional clades: Plasma membrane, endosomal, and vacuole classes (Yokoi *et al.* 2002). AtNHX1–6 operate in vacuoles or endosomal regions to transport $Na^+$ or $K^+$ in exchange for $H^+$ to the cytosol (Mäser *et al.* 2001). AtNHX7 (Salt Over Sensitive 1, SOS1) and AtNHX8 function at the plasma membrane, and SOS1 plays a key role in mediating $Na^+$ efflux in the root and transporting $Na^+$ in the vacuole (Shi *et al.* 2002). NHXs have been identified in many plants, including 8 in *Arabidopsis*, grape, and poplar, and 7 in rice, sorghum, maize, *Medicago truncatula*, and wheat (Mäser *et al.* 2001; Li *et al.* 2024). Plasma membrane High-affinity potassium transporters (HAK) play a vital role in $K^+$ uptake and transport and are essential for maintaining $Na^+/K^+$ homeostasis in plants (Munns and Tester 2008), such as AtHAK5 in *Arabidopsis*, HvHAK1 in barley (*Hordeum vulgare*), OsHAK1 and OsHAK5 in rice, and CaHAK1 in pepper (*Capsicum annum*) (Martínez-Cordero *et al.* 2004; Yang *et al.* 2014; Chen *et al.* 2015). Some members of HAK also play important roles in $Na^+$ and $Cs^+$ transport, such as ZmHAK4 and ZmHAK17 in maize and SlHAK20 in tomato (Zhang *et al.* 2019; Wang *et al.* 2020; Wang *et al.* 2024).

Blueberries are a highly nutritious perennial fruit crop with a shallow root system and lack of root hairs, making them highly sensitive to soil salinity (Kalt *et al.* 2020; Bryla *et al.* 2021). Soil salinization leads to $Na^+$ and $Cl^-$ accumulation in blueberry leaves, resulting in osmotic stress and ionic toxicity, which decreases photosynthetic capacity and eventually causes wilting (Muralitharan *et al.* 1990; Song *et al.* 2023). The molecular regulation mechanisms of blueberry salinity tolerance identified so far include the basic leucine zipper factor (*VabZIP12*), peroxisomal ion protease (*VcLON1*, *VcLON2*), and the $Na^+$-transporter *VcHKT1;1*, all of which contribute to salt tolerance in blueberry (Muralitharan *et al.* 1990; Chen *et al.* 2017; Zhong *et al.* 2019; Qu *et al.* 2022; Song *et al.* 2023). However, a comprehensive understanding of blueberries' response to salt stress remains limited, and it is essential to identify the key factors that regulate variations in salt tolerance to develop salt-tolerant cultivars.

Grafting is a traditional horticultural technique that reduces ionic stress in shoots by using salt-tolerant rootstocks to limit the transfer of $Na^+$ and $Cl^-$ from roots to the scion (Estañ *et al.* 2005; Henderson *et al.* 2018). Various genes were identified for regulating ion transport in both rootstocks and leaves, such as the grapevine (*Vitis vinifera*) *VisHKT1;1*, and peach (*Prunus persica*) *PpHKT1*, that confer shoot $Na^+$ exclusion to scions (Henderson *et al.* 2018; Kaundal *et al.* 2019). Our previous research found that *VcHKT1;1* is a root-specific expressed gene in blueberry, promotes $Na^+$ exclusion in leaves, and enhances salt tolerance (Song *et al.* 2023). However, the salt tolerance of *antiVcHKT1;1*$^{DK}$ (knockdown of *VcHKT1;1* in 'Duke') is intermediate between the salt-sensitive cultivar 'Sweetheart' and the salt-tolerant cultivar 'Duke'. To explore the genetic and physiological basis of salt tolerance in blueberries, we performed Gene Ontology (GO) and weighted gene co-expression network analysis (WGCNA), focusing on identifying regulatory pathways and key genes involved in ion transport and homeostasis. Additionally, the study investigates the potential of grafting with salt-tolerant rootstocks as a practical approach to mitigate salt stress. These findings will provide valuable insights into the molecular mechanisms underlying salt stress adaptation in blueberries and offer actionable targets for breeding and sustainable cultivation practices.

## 2. Materials and methods

### 2.1. Plant materials, growth conditions, and salt treatment

Salt tolerance was compared among highbush blueberry with the salt-sensitive cultivar 'Sweetheart' (SH), the salt-tolerant cultivar 'Duke' (DK), and the mutant (*antiVcHKT1;1*$^{DK}$) with the knockdown of *VcHKT1;1* in DK. The plants were grown under a 16-h light/8-h dark cycle at 25°C. Pots (5 cm diameter, 8 cm height) were filled with a substrate mix of natural peat soil and vermiculite in a 1:1 ratio. Uniform 3-month-old seedlings were watered with a 150 mmol $L^{-1}$ NaCl solution until the soil was saturated, with water as the control treatment. The leaf samples were collected to measure $Na^+$ and $K^+$ contents. For transcriptome analysis, two-year-old blueberry plants (~25 cm in height) were grown under controlled conditions. The plants received a single 200 mmol $L^{-1}$ NaCl treatment, with water as the control treatment. Photos were taken at 0, 3, 12, 24, 48, and 72 h after salt treatment, and leaves and roots were collected at these time points for $Na^+$ and $K^+$ contents measurements, sequencing, and reverse transcription quantitative PCR (qRT-PCR) validation. Five plants were used for each treatment, with three biological repeats per group.

### 2.2. Measurement of $Na^+$ and $K^+$ content

$Na^+$ and $K^+$ contents were measured using a method previously described (Huang *et al.* 2020). Samples were dried at 80°C for 24 h and ground into powder, and $Na^+$ and $K^+$ contents were measured using inductively coupled plasma optical emission spectrophotometry (Teledyne Leeman Labs, Prodigy 7, USA). The contents of $Na^+$ and $K^+$ were calculated using a previously described method based on the samples' dry weight and the measured concentrations (Song *et al.* 2023).

### 2.3. RNA extraction, sequencing, and RNA-sequencing (RNA-seq) analysis

Leaves and roots were collected at 3 and 12 h under salt treatment, a total of 48 samples. The cDNA library was constructed at Majorbio Bio-pharm Biotechnology Co., Ltd. (Shanghai, China) using IlluminaÒ Stranded mRNA Prep, Ligation (San Diego, CA), and the SMART-Seq-V4 Ultra Low Input RNA Kit for sequencing. Raw reads were processed with fastp for trimming and quality control, generating approximately 6.04 GB of clean data per sample. Based on RNA-seq results, clean reads were aligned to the blueberry reference genome *Vaccinium corymbosum* cv. Draper v1.0 uses HiSat2 software, which is accessible at vaccinium.org (Colle *et al.* 2019). Gene expression levels were quantified using RSEM (version 1.2.31) based on the FPKM (fragments per kilobases of transcript per million mapped reads) method. DESeq2 software (version 1.10.1) was employed to identify differentially expressed genes (DEGs) between control and salt treatment, with a *P*-value<0.05. DEGs were defined by a fold change (FC)≥3 and a false discovery rate (FDR)<0.05. GO enrichment analysis was performed using Goatools, with a significance threshold of $P \leq 0.05$. All raw sequencing data were submitted to the National Center for Biotechnology Information database.

### 2.4. WGCNA

WGCNA was performed to identify candidate genes, following default parameters as previously described (Zhong *et al.* 2022). The analysis was conducted using the WGCNA package (https://horvath.genetics.ucla.edu/html/CoexpressionNetwork/Rpackages/WGCNA/). Ion transport and homeostasis genes with a mean FPKM of at least 1.0 and a variance greater than 1.0 were selected for clustering. The module parameters were set: networkType=signed, soft power=12, minModuleSiza=30, minKMEtoStay=0.3, and mergeCutHeight=0.25. A weighted co-expression network was then constructed, grouping thousands of genes into color modules. Correlations between the characteristic genes of these modules and $Na^+/K^+$ contents or sample traits were calculated. Each module network and hub genes were visualized using Cytoscape (v.3.7.2).

### 2.5. qRT-PCR analysis

Approximately 1 μg of RNA was used for cDNA synthesis using 5× All-In-One RT MasterMix (Biological Materials Inc., Vancouver, BC, Canada). qRT-PCR was conducted with PowerUp™ SYBR™ Green Master Mix (Thermo Fisher Scientific, Waltham, MA, USA) on a StepOne Plus Real-Time PCR System (ABI, Vernon, CA, USA) following the manufacturer's protocol. *VcUBC28* served as an internal reference gene (Vashisth *et al.* 2011), and transcript levels were calculated by the $2^{-\Delta\Delta Ct}$ method. Primer sequences are listed in Appendix A, and each qRT-PCR assay was performed with three replicates.

### 2.6. Subcellular localization analysis of VcHAK5, VcNHX1, and VcNHX2

*VcHAK5*, *VcNHX1*, and *VcNHX2* coding sequences were inserted into the pCAMBIA1300-GFP vector. The pCAMBIA1300-VcHAK5-GFP construct was co-transformed with AtCBL1-OFP into *Nicotiana benthamiana* protoplasts, with AtCBL1 as a plasma membrane marker (Batistic *et al.* 2008). For VcNHX1 and VcNHX2, pCAMBIA1300-VcNHX1-GFP and pCAMBIA1300-VcNHX2-GFP constructs were co-transformed with Atγ-TIP-mCherry, a tonoplast-localized marker (Liang *et al.* 2023). Fluorescent signals were observed with a Carl Zeiss LSM780 confocal laser microscope. Primer sequences are provided in Appendix A.

### 2.7. Yeast complementation

*VcHAK5*, *AtHKT1*, and *AtHAK5* were inserted into the p416-GPD vector and transformed into the yeast strains *ant5* and *trk1 trk2* (Calero *et al.* 2000; Quintero *et al.* 2002; Li *et al.* 2017). The yeast cells were cultured and grown following the described research (Qin *et al.* 2019; Zhang *et al.* 2019). Cells were serially diluted in 10-fold increments and grown in AP medium with varying concentrations of NaCl and KCl, then incubated at 30°C for 2–3 d to evaluate growth. *VcNHX1*, *VcNHX2*, and *AtNHX1* were conducted in the pDR195 vector and introduced into the yeast strain *Δnhx1*. The method followed was previously described (Gaxiola *et al.* 1999; Li *et al.* 2024).

### 2.8. Generation of the *VcHAK5*, *VcNHX1*, and *VcNHX2* RNAi-silenced calli

The RNAi fragments of *VcHAK5*, *VcNHX1*, and *VcNHX2* were inserted into the pRI-RNAi vector, which contains a chsA intron and the 35S CaMV promoter (Song *et al.* 2013; Chen *et al.* 2019; Xu *et al.* 2020). The recombinant vectors (RNAi-*VcHAK5*, RNAi-*VcNHX1*, and RNAi-*VcNHX2*) were transformed into *Agrobacterium tumefaciens* strain EHA105. Blueberry calli were subjected to *Agrobacterium*-mediated transformation according to established protocols (Qin *et al.* 2023). Transgenic calli were confirmed through qRT-PCR analysis. Blueberry calli at 20 days old were cultured on medium with 150 mmol $L^{-1}$ NaCl for 5 d, then photographed, and their fresh weight, $Na^+$, and $K^+$ contents were measured.

### 2.9. Grafting experiment and salt treatment

One-year-old blueberry seedlings of SH and DK were used for the reciprocal grafting experiment. The grafted combinations included SH as the rootstock, DK as the scion (DK/SH), and DK as the rootstock with SH as the scion (SH/DK), with 10 replicates. After 30 d of growth under controlled environmental conditions. Plants were watered once with 200 mmol $L^{-1}$ NaCl until the soil was saturated; the control was watered. Three days later, plants were photographed, and leaves were collected for $Na^+$ and $K^+$ analysis.

### 2.10. Measurements of chlorophyll fluorescence

The chlorophyll fluorescence was measured on the third or fourth fully developed leaves using a PEA (Hansatech, UK), and each treatment was repeated three times. The minimum fluorescence ($F_o$), maximum fluorescence ($F_m$), and the maximum quantum yield of PSII ($F_v/F_m=(F_m-F_o)/F_m$) were calculated (Coba de la Peña *et al.* 2010).

### 2.11. Accession numbers

Sequence data from this article can be found in the GenBank/EMBL data libraries under accession numbers found in Appendix B. The RNA-seq data have been deposited in the NCBI database (https://submit.ncbi.nlm.nih.gov/subs/sra/SUB14744964), BioProject PRJNA1164779.

### 2.12. Statistical analysis

All statistical analyses were conducted in GraphPad Prism v.8.0.2 for Windows (GraphPad Software, La Jolla, CA, USA). Data are reported as mean±SD, with statistical tests specified in the corresponding figure legends.

## 3. Results

### 3.1. Comparative analysis of salt tolerance in blueberry cultivars SH and DK and *antiVcHKT1;1*$^{DK}$

The highbush blueberry cultivars SH and DK display notable differences in salt tolerance. The *antiVcHKT1;1*$^{DK}$ is a *VcHKT1;1* knockdown mutant in the salt-tolerant cultivar DK that exhibits salt sensitivity and higher leaf $Na^+$ content than DK under salt stress (Song *et al.* 2023). Here, we further compared the salt tolerance of the blueberry cultivars SH, DK, and the *antiVcHKT1;1*$^{DK}$ mutants, and found that the salt tolerance of *antiVcHKT1;1*$^{DK}$ is intermediate between that of SH and DK (Fig. 1-A–C). Under salt treatment, SH showed the highest salt sensitivity, with leaves turning almost completely yellow. The *antiVcHKT1;1*$^{DK}$ phenotype displayed intermediate sensitivity, with partial leaf yellowing, while DK showed only a slight change in color at the leaf margins. All plants grew well under normal conditions (Fig. 1-A). The $Na^+$ content revealed that SH leaves accumulated nearly threefold higher $Na^+$ compared to DK. The $Na^+$ contents in *antiVcHKT1;1*$^{DK}$ mutants were intermediate between SH and DK, with DK leaves showing the least $Na^+$. The $Na^+/K^+$ ratios followed a similar trend, with no differences under normal conditions (Fig. 1-B and C). These results suggest that the difference in salt tolerance between the blueberry cultivars SH and DK is not only a result of the regulation of the transport gene *VcHKT1;1*, but may also involve other key salt tolerance genes.

### 3.2. A comprehensive analysis of salt tolerance differences between blueberry cultivars SH and DK

To comprehensively compare salt tolerance between the blueberry cultivars SH and DK, we continuously recorded salt stress phenotypes over 72 h under 200 mmol $L^{-1}$ NaCl treatment (Fig. 1-D–H). After 24 h of salt treatment, the leaves of SH began to turn yellow, particularly the older and top young leaves, followed by wilting and apoptosis as salt stress continued (indicated by red arrows in Fig. 1-D). In contrast, DK exhibited a mild yellowing phenotype only after 48 h of salt stress (Fig. 1-D). A decrease in the $F_v/F_m$ value indicated damage to photosystem II. After just 3 h of salt treatment, the $F_v/F_m$ values of SH showed a particular decline. As the treatment progressed, photosystem II in SH was seriously affected compared to DK (Fig. 1-E). Meanwhile, the accumulation of $Na^+$ and $K^+$ for salt treatment also showed distinct differences between the two cultivars (Fig. 1-F–H). A significant difference in $Na^+$ content appeared after 12 h of salt stress, with $Na^+$ accumulation in the leaves gradually increasing as salt stress continued. The relative increase in DK was slower than in SH (Fig. 1-F). Similar differences were observed in $K^+$ content and $Na^+/K^+$ ratio between the two cultivars under salt stress (Fig. 1-G and H). These results suggest that the differences in salt sensitivity among blueberry cultivars are closely related to $Na^+$ content and $Na^+/K^+$ homeostasis in the leaves under salt stress.

To analyze global gene expression differences in the blueberry cultivars SH and DK under salt treatment, we examined differentially expressed genes (DEGs) in the leaves and roots of both cultivars after 3 and 12 h of salt treatment (Fig. 2; Appendices C and D). Transcriptome reads were aligned to the blueberry genome version 1.0 (http://gigadb.org/dataset/100537), with an average of 40 million mapped reads per library (Appendix D). A principal component analysis (PCA) assessed the relationship and variation among the sample replicates (Appendix C). The number analysis of DEGs revealed that more DEGs were present in both cultivars at 12 h of salt treatment compared to 3 h (Fig. 2). Additionally, more than twice as many DEGs were found in the roots as in the leaves (Fig. 2-A). The Venn diagrams showed that after 3 and 12 h of salt treatment, SH had 2,153 shared DEGs in the roots, while DK had 3,019; in the leaves, the numbers were 710 and 1,508, respectively (Fig. 2-B). These results indicated that the response to salt stress in blueberry becomes complex and diverse between roots and leaves tissues.

### 3.3. Ion transport and ion homeostasis pathways were enriched in response to salt stress

To further analyze gene expression differences between tissues in SH and DK, we classified the DEGs into tissue-specific or shared expression patterns. The results showed that 17,872 genes, accounting for 59.62% of the total DEGs, were specifically expressed in the roots of both cultivars (Fig. 3-A). Of these, 26.14% were specific to the root of SH (SH_R), while 20.10% were specific to DK roots (DK_R), and 13.38% were shared between the two cultivars. In addition, fewer DEGs were observed in the leaves, with 6,212 genes being leaf-specific, accounting for 20.72% of the total DEGs. Specifically, 7.12% of the DEGs were unique to SH leaves (SH_L), 11.06% were unique to DK leaves (DK_L), and 2.54% were shared between the two cultivars (Fig. 3-A).

GO enrichment analysis was conducted for tissue-specific and shared DEGs in roots and leaves (Fig. 3-B). DEGs specific to SH_R were significantly enriched in GO terms such as “ion transport”, “hormone-mediated signaling pathway”, and “lignin catabolic process”. Similarly, DK_R-specific DEGs were enriched in terms like “ion transport”, “cellular ion homeostasis”, and “protein phosphorylation”. For SH_L and DK_L-specific DEGs, the enrichment focused on Go terms related to “ion transport” and “response to biotic stimulus” (Fig. 3-B). Additionally, DEGs shared in roots were enriched in “response to stimulus”, “ion transport”, and “cellular ion homeostasis”. While shared DEGs in leaves were enriched in “response to stimulus” and “ion transport”. DEGs shared

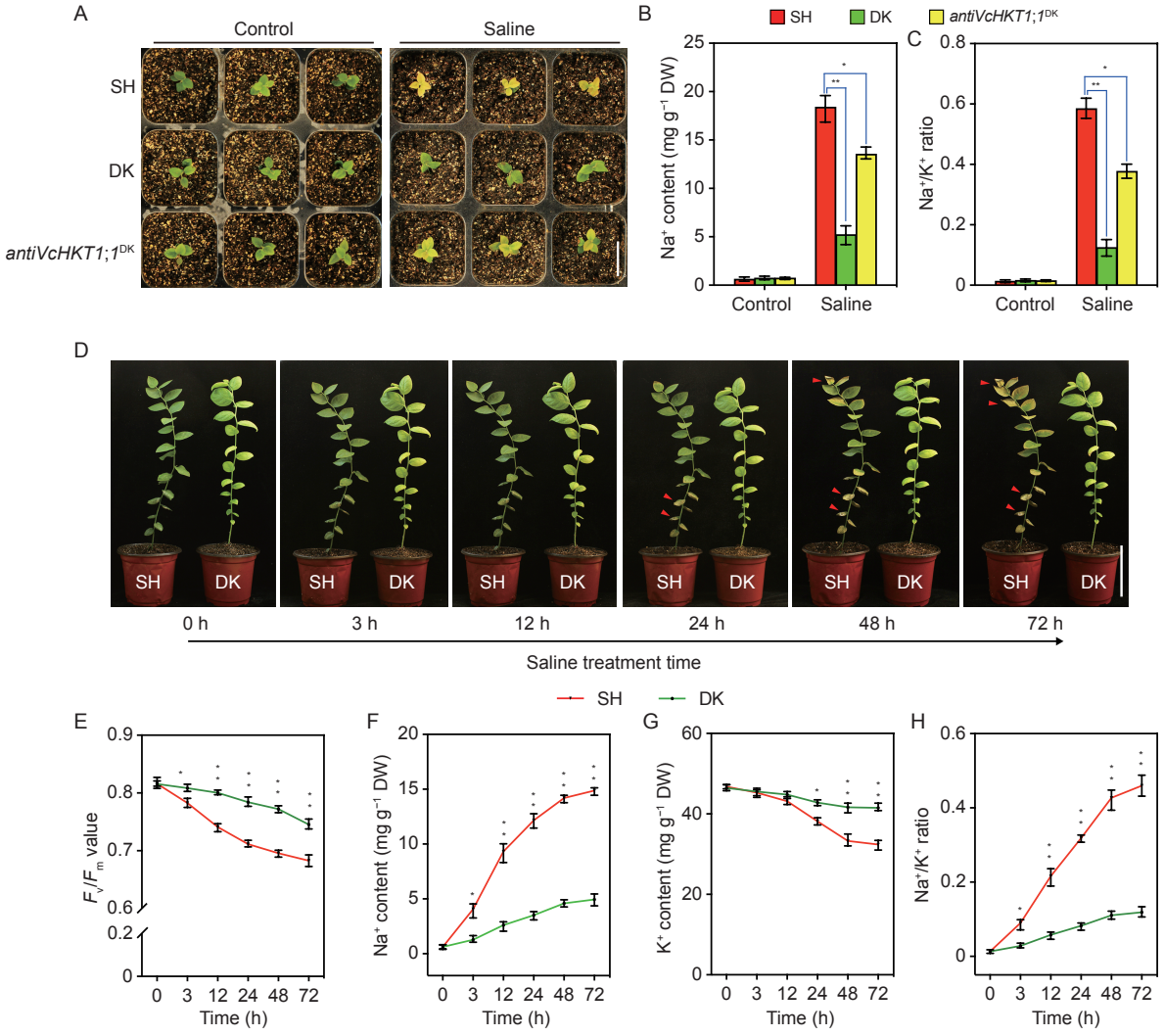



**Fig. 1 The salt tolerance of the knockdown mutant *antiVcHKT1;1*$^{DK}$ is intermediate between 'Sweetheart' (SH) and 'Duke' (DK).** A, phenotypes of the salt-sensitive SH, the salt-tolerant DK, and the knockdown mutant (*antiVcHKT1;1*$^{DK}$) under control and salt treatment conditions. Three-month-old seedlings were treated with 150 mmol $L^{-1}$ NaCl for 3 d. Scale bar=2 cm. B and C, leaf $Na^+$ content (B) and $Na^+/K^+$ ratio (C) in SH, DK, and *antiVcHKT1;1*$^{DK}$ under salt treatment and control. DW, dry weight. D, phenotypic changes under persistent salt stress at six time points (0, 3, 12, 24, 48, and 72 h) in SH and DK, scale bar=10 cm. E–H, $F_v/F_m$ value (E), $Na^+$ content (F), $K^+$ content (G), and $Na^+/K^+$ ratio (H). Data in B, C and E–H are represented as mean±SD of three replicates. Statistical analyses were performed using two-way ANOVA (B and C) and multiple *t*-tests (E–H). Significant differences are indicated by asterisks, $^*$, $P<0.05$; $^{**}$, $P<0.01$.

between both roots and/or leaves showed enrichment in "ion transport" and "response to abiotic stimulus" (Fig. 3-B). These findings suggest that root-specific DEGs may play a critical role in regulating the differences in salt stress responses between blueberry cultivars SH and DK. The pathways "ion transport" and "ion homeostasis" are likely crucial for the differential salt stress responses in these cultivars.

### 3.4. Hub genes identified through weighted gene co-expression network

WGCNA was performed to identify hub genes involved in the pathways "ion transport" and "ion homeostasis", which were correlated with $Na^+$ and $K^+$ contents as well as $Na^+/K^+$ ratio in SH and DK (Fig. 4). The identified genes were divided into 13 modules (Fig. 4-A; Appendices E and F). The eigengene-trait correlation analysis showed the MEyellow module had 198 genes that were highly correlated with $K^+$ content (correlation coefficient=0.893, *P*-value=0), and the MEmagenta module contained 163 genes that were significantly associated with $Na^+$ content (correlation coefficient=0.543, *P*-value=0.0163) (Fig. 4-B; Appendix F). MEgrey and MEbrown were lowly correlated with $Na^+$, $K^+$, and $Na^+/K^+$ ratio (Fig. 4-B; Appendix G). Additionally, MEyellow and MEmagenta modules showed high correlations in roots and leaves (Appendix E). A co-expression network of the MEyellow and MEmagenta modules was conducted, consisting of 25 genes with correlation values greater than 0.5 and $P<0.05$ (Fig. 4-C). Among these, *VcHAK5*, *VcNHX1*, *VcNHX2*, *VcHKT1;1*, *VcHAK1*, *VcHAK26*, *VcCHX20;1*, and *VcCHX20;2* predictably participated in $Na^+/K^+$ transport, and the remaining 17 genes were primarily associated with the transport of metal ions such as iron, copper, and zinc *via* GO enrichment analysis (Appendix B). A Venn analysis revealed the distribution of these $Na^+/$

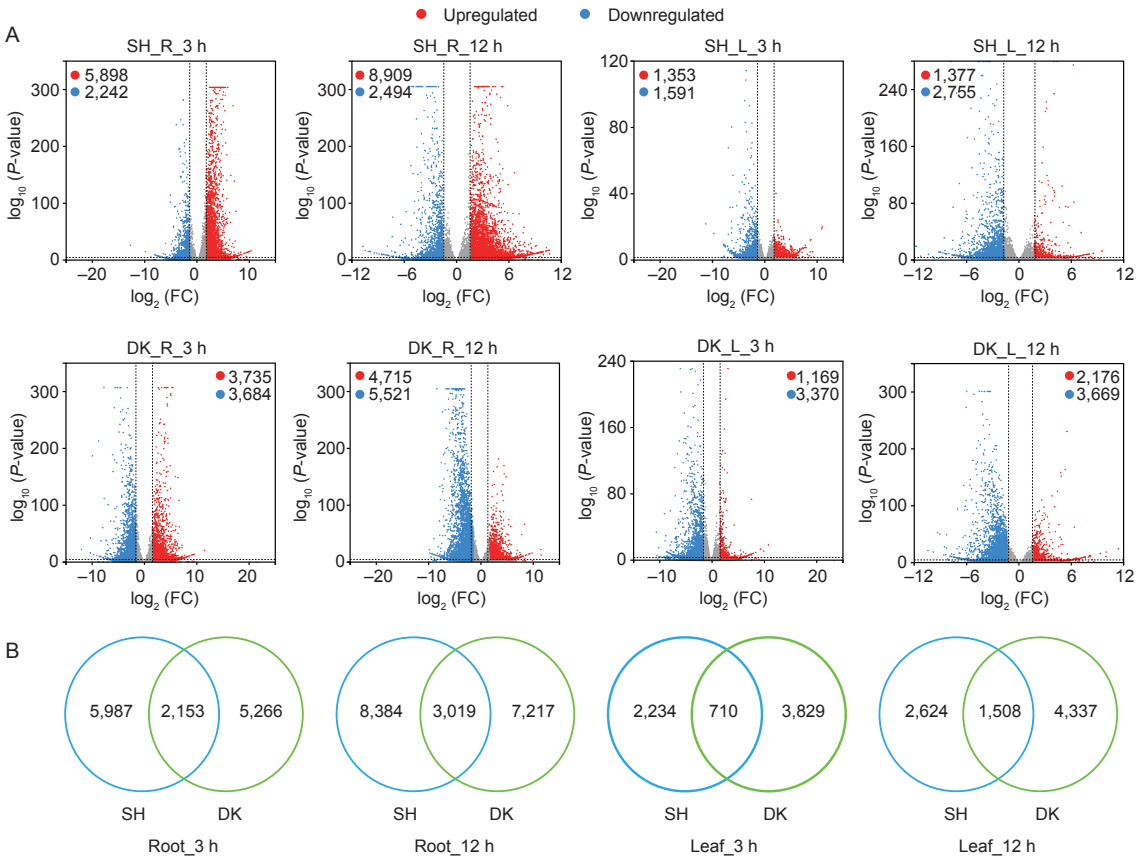



**Fig. 2 Global gene expression changes in blueberry cultivars 'Sweetheart' (SH) and 'Duke' (DK) under salt treatment.** A, volcano plots showing the fold change of differentially expressed genes (DEGs) under salt treatment compared to control conditions. Samples included roots of SH (SH_R) and DK (DK_R), and leaves of SH (SH_L) and DK (DK_L), collected at 3 and 12 h of salt treatment. DEGs were defined by a fold change≥3 and a *P*-value<0.05. Red, blue, and gray dots represent genes with upregulated, downregulated, and no significant changes in expression, respectively. Three independent experiments for each sample. B, Venn diagrams showing the shared and unique DEGs between SH and DK in roots and leaves under salt treatment at 3 and 12 h, respectively.

$K^+$ transport-associated genes in SH and DK roots (Fig. 4-D). *VcHAK5*, *VcNHX1*, *VcNHX2*, and *VcHKT1;1* especially differently expressed in the roots of DK, *VcHAK1*, *VcCHX20;1* and *VcCHX20;*2 expressed in both SH and DK. *VcHAK26* in SH roots (Fig. 4-D). The expression levels of these genes were further validated using RNA-seq and qRT-PCR analyses (Fig. 5; Appendix H). These results showed that *VcHAK5*, *VcNHX1*, and *VcNHX2* were significantly up-regulated in blueberry roots and minimally expressed in leaves. Notably, their expression in DK roots under salt stress increased by more than 3-fold, while no significant regulation was observed in SH.

### 3.5. VcHAK5, VcNHX1 and VcNHX2 exhibit different $Na^+$ and $K^+$ transport activities

A phylogenetic analysis of blueberry VcHAK5, VcNHX1, and VcNHX2, along with *Arabidopsis* HAKs and NHXs, revealed that VcHAK5 clustered with AtHAK5, sharing 53.8% amino acid identity and a highly conserved protein structure (Appendices I and J). VcHAK5 featured 11 putative transmembrane domains as predicted by TMHMM (Appendices I and K). Similarly, VcNHX1 and VcNHX2 clustered with AtNHX1 and AtNHX2, sharing more than 50% amino acid identity with them and containing 12 and 11 putative transmembrane domains, respectively (Appendices I and K). Subcellular localization revealed that the VcHAK5-GFP fusion protein co-localized with AtCBL1-OFP, a plasma membrane marker (Batistic *et al.* 2008). VcNHX1-GFP and VcNHX2-GFP fusion proteins co-localized with the tonoplast marker Atγ-TIP-mCherry (Liang *et al.* 2023) in *N. benthamiana* protoplasts (Fig. 6-A and B). These findings indicated that VcHAK5 is localized to the plasma membrane, while VcNHX1 and VcNHX2 are localized to the tonoplast.

Functional expression assays were performed using yeast mutant strains to determine the $Na^+$ and $K^+$ selectivity of VcHAK5, VcNHX1, and VcNHX2 (Fig. 6-C–F). Since VcHAK5 localized to the plasma membrane (Fig. 6-A), the yeast strain *ant5*, deficient in plasma membrane $Na^+$ exclusion (Quintero *et al.* 2002), and the *trk1 trk2* strain, lacking plasma membrane $K^+$ uptake capacity (Calero *et al.* 2000), were used for ion-selectivity testing. *Ant5* cells expressing *AtHKT1*, a $Na^+$-selective transporter (Davenport *et al.* 2007), exhibited a salt-sensitive phenotype under >25 mmol $L^{-1}$ NaCl, with growth inhibition increasing as NaCl concentration rose. In contrast, *ant5* cells expressing *VcHAK5* showed growth comparable to empty vector controls (Fig. 6-C). Similarly, *trk1 trk2* cells

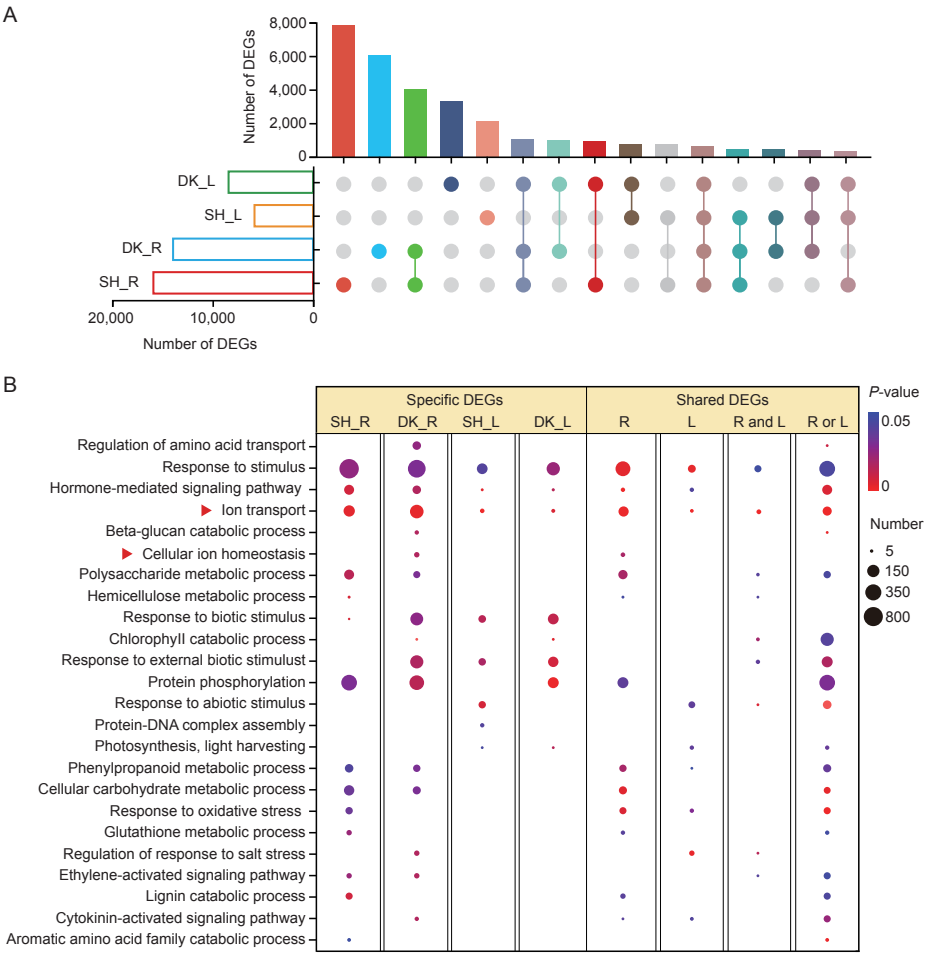



**Fig. 3 Venn diagram and enrichment analyses with differentially expressed genes (DEGs) responding to salt stress in blueberry.** A, upset plot (an alternative to a Venn diagram) showing the overlap and count of DEGs across four groups: SH roots (SH_R), DK roots (DK_R), SH leaves (SH_L), and DK leaves (DK_L). The bar plot at the top shows the total number of DEGs in each group, and the matrix below shows the intersections. B, Gene Ontology (GO) enrichment analysis for both specific and shared DEGs in the roots (R) and leaves (L) of SH and DK. Specific DEGs were identified in individual tissues and cultivars (SH_R, DK_R, SH_L, and DK_L), and shared DEGs were those expressed in both SH and DK in either roots or leaves. The color of the points represents the *P*-values for each GO term, ranging from red (high enrichment) to blue (low enrichment), while their size corresponds to the number of genes. The red triangles refer to the GO terms related to ion transport and cellular ion homeostasis.

expressing *VcHAK5* or *AtHAK5*, a $K^+$-selective transporter (Ródenas *et al.* 2021), restored growth in media containing 0.1–1.0 mmol $L^{-1}$ $K^+$ (Fig. 6-D). These results indicate that VcHAK5 facilitates $K^+$ transport but not $Na^+$. In addition, the $Na^+$ and $K^+$ selectivity of VcNHX1 and VcNHX2 as transporters were demonstrated by complementation assays in the yeast strain Δ*nhx1* (Fig. 6-E and F). The strain Δ*nhx1*, deficient in the *ScNHX1* gene, showed strong growth inhibition under high $Na^+$ and $K^+$ conditions (Venema *et al.* 2002; Apse *et al.* 2003). However, Δ*nhx1* cells transformed with VcNHX1 and VcNHX2 exhibited significantly improved growth under 200 mmol $L^{-1}$ NaCl or 800 mmol $L^{-1}$ KCl, although full recovery was not achieved. A similar growth pattern was observed in Δ*nhx1* cells expressing AtNHX1 (Fig. 6-E and F).

### 3.6. Knockdown of *VcHAK5*, *VcNHX1* and *VcNHX2* reduces salt tolerance in blueberry

To investigate the roles of *VcHAK5*, *VcNHX1*, and *VcNHX2* in regulating salt tolerance in blueberry, we generated RNAi-mediated knockdown blueberry calli for each gene. The expression levels of *VcHAK5*, *VcNHX1*, and *VcNHX2* were significantly reduced in the RNAi blueberry calli compared to the wild type (Appendix L). The RNAi blueberry calli exhibited increased salt sensitivity, with blueberry calli turning yellow under 150 mmol $L^{-1}$ NaCl treatment (Fig. 7-A). After 5 d of salt treatment, the fresh weight of RNAi blueberry calli (RNAi-*VcNHX1*, and RNAi-*VcNHX2*) decreased by 50%, 60%, and 58%, respectively, compared with the control (Fig. 7-B). Furthermore, the RNAi blueberry calli showed a marked increase in $Na^+$ content and $Na^+/K^+$ ratios, along with a substantial decrease in $K^+$ content under salt treatment conditions, with no significant in control conditions (Fig. 7-C–E). These results suggest that VcHAK5, VcNHX1, and VcNHX2 play an important role in regulating $Na^+$ homeostasis and the $Na^+/K^+$ ratio, contributing to blueberry salt tolerance.

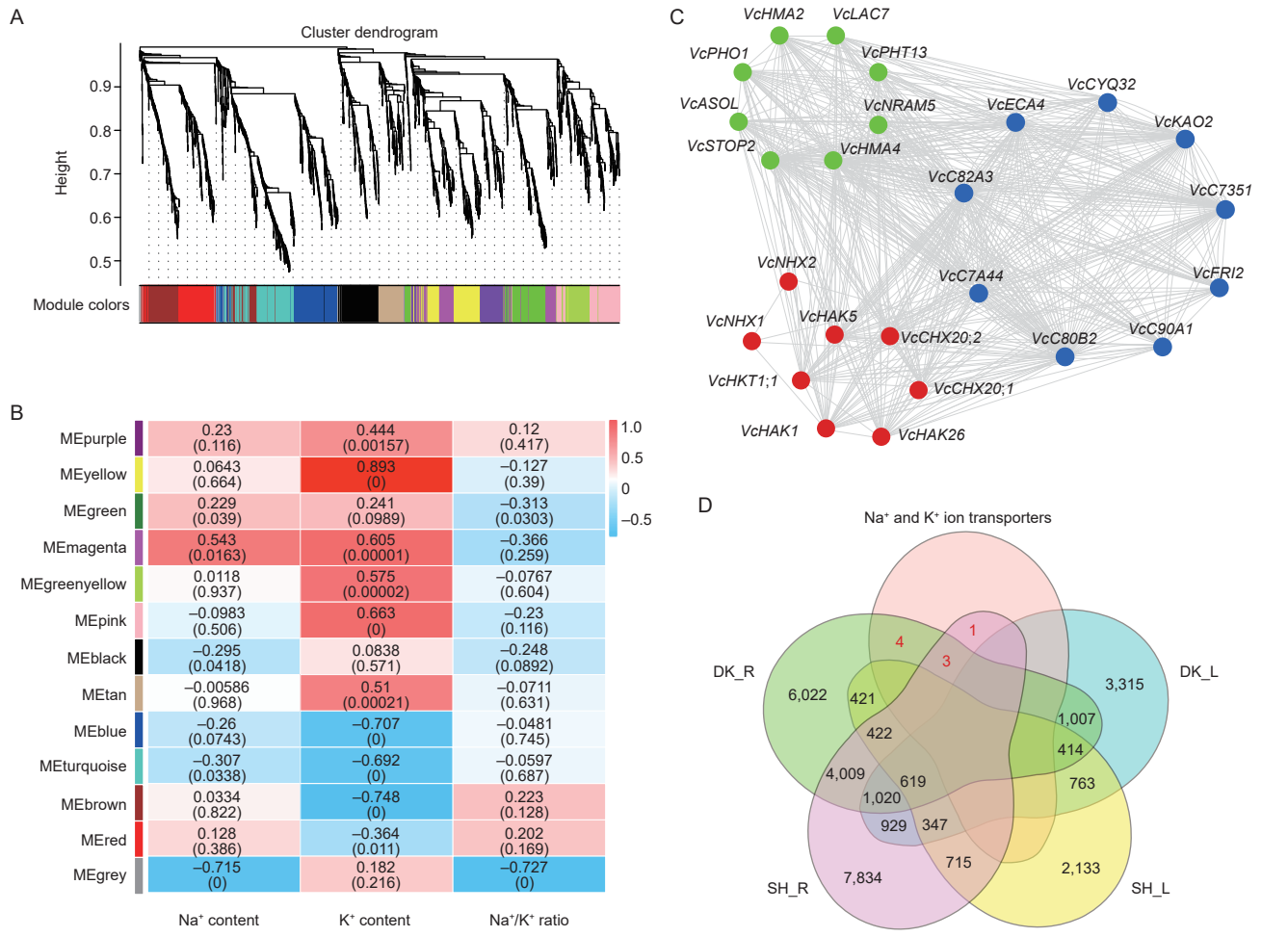



**Fig. 4 Weighted gene co-expression network analysis (WGCNA) to identify hub genes associated with salt stress responses in blueberry.** A, the hierarchical cluster dendrogram showing co-expressed modules identified by WGCNA. Each leaf on the tree represents one gene. The major branches form 13 modules (based on a threshold of 0.25), each labeled with a distinct color. B, heatmap showing correlations between co-expression modules (vertical axis) and traits (horizontal axis). The colors of the squares range from red (indicating a positive correlation) to blue (indicating a negative correlation). Values in each square represent the correlation coefficient, with *P*-values in parentheses. C, the top 25 hub genes of the co-expression network from the MEyellow and MEmagenta modules responding to salt stress. Genes related to $Na^+$ and $K^+$ transport are marked with red. The functions of the other genes are described in Appendix B. D, Venn diagrams showing the overlap between $Na^+/K^+$ ion transport-related genes and the total DEGs in four groups (DK_R, SH_R, DK_L, and SH_L).

### 3.7. Grafting with salt-tolerant rootstocks contributes to enhancing blueberry salt tolerance

To further clarify blueberry roots contributed to salt tolerance by reducing leaf $Na^+$ accumulation, we conducted reciprocal grafting experiments between the SH and DK cultivars, ensuring that the original genetic traits aboveground remained unaltered (Fig. 8). The reciprocal grafting was performed using one-year-old seedlings of SH and DK. Seedlings of SH, DK, DK/SH (grafting SH as rootstock), and SH/DK (grafting DK as rootstock) grew well under uniformly controlled conditions (Fig. 8-A). Under these conditions, there were no significant differences in $F_v/F_m$ values, leaf $Na^+$ contents, $K^+$ contents, and $Na^+/K^+$ ratios among the groups (Fig. 8-B–E). However, the SH cultivar under soil salt stress showed a salt-sensitive phenotype, characterized by decreased $F_v/F_m$ values compared to the salt-tolerant DK cultivar. These findings are consistent with the results shown in Fig. 1-D and E. Similarly, seedlings with SH as rootstock (DK/SH) also displayed a salt-sensitive phenotype and reduced $F_v/F_m$ values, mirroring the SH response. In contrast, seedlings with DK as rootstock (SH/DK) exhibited a salt-tolerant phenotype similar to that of DK (Fig. 8-A). Notably, under salt stress, plant with SH roots (SH and DK/SH) exhibited significantly higher leaf $Na^+$ contents and $Na^+/K^+$ ratios, but lower leaf $K^+$ contents, than plants with DK roots (DK and SH/DK) (Fig. 8-C–E). These results presented here indicated that blueberry roots play a critical role in salt tolerance by modulating leaf $Na^+$ accumulation and maintaining a favorable $Na^+/K^+$ ratio.

## 4. Discussion

Blueberry was susceptible to salinity due to its complex ploidy, lengthy growth cycle, and shallow roots without root hairs (Colle *et al.* 2019; Wang *et al.* 2022; Yang *et al.* 2022). Leaf $Na^+$ content variations are associated with varying levels

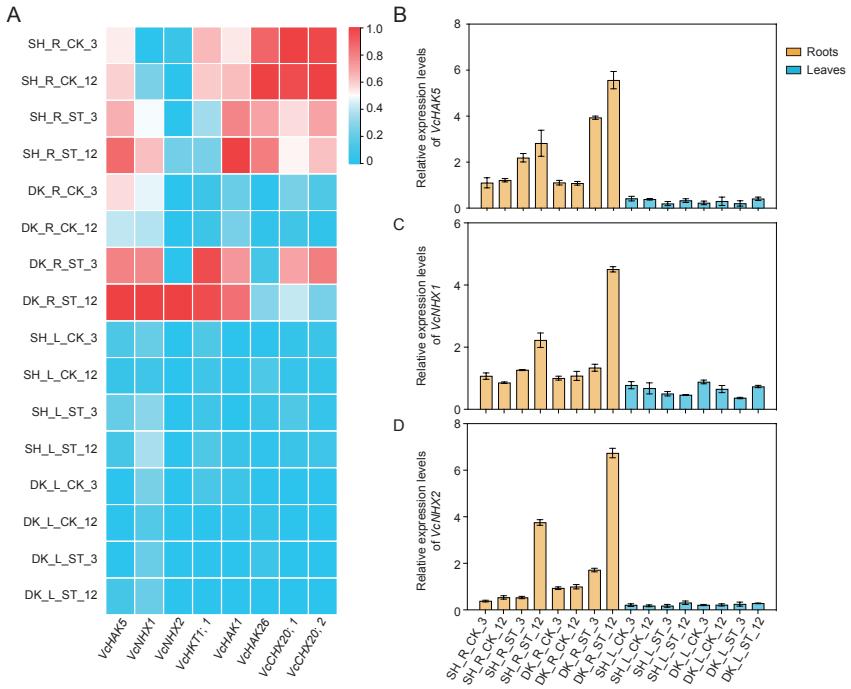



**Fig. 5 The expression levels of potential $Na^+$ and $K^+$ transport genes.** A, heatmaps displaying the transcription levels of $Na^+$ or $K^+$-related transport genes (*VcHAK5*, *VcNHX1*, *VcNHX2*, *VcHKT1;1*, *VcHAK1*, *VcNHAK26*, *VcCHX20;1*, and *VcCHX20;2*) in the different samples, ranging from upregulated (red) to downregulated (blue). The expression levels of the DEGs are shown using a z-score-normalized color scale; blue indicates low expression and red indicates high expression. The transcript sequencing data for each sample are based on three replicates. B–D, qRT-PCR analysis of the hub genes *VcHAK5*, *VcNHX1*, and *VcNHX2* in blueberry cultivars 'Sweetheart' and 'Duke', respectively. The qRT-PCR analysis for *VcHKT1;1*, *VcHAK1*, *VcNHAK26*, *VcCHX20;1*, and *VcCHX20;2* is presented in Appendix H. Data were the mean±SD and three independent replicates. SH, 'Sweetheart'; DK, 'Duke'; R, root; L, leaf; CK, control; ST, salt treatment; 3 and 12, 3 and 12 h under salt treatment.

of salt tolerance in blueberry cultivars. Comprehensive insights into blueberry responses to salt stress, identifying target genes for enhancing salt tolerance, and highlighting the importance of salt-resistant rootstocks are crucial for enhancing salt tolerance in blueberries. The *VcHKT1;1* was involved in leaf $Na^+$ exclusion and played a key role in salt tolerance. The *antiVcHKT1;1*$^{DK}$ mutant (a *VcHKT1;1* knockdown mutant) accumulates more $Na^+$ in its leaves, leading to greater sensitivity to salt stress (Song *et al.* 2023). In this study, we compared $Na^+$ content and $Na^+/K^+$ ratio in the leaves of a salt-sensitive cultivar, SH, a salt-tolerant cultivar, DK, and a mutant *antiVcHKT1;1*$^{DK}$. We found that the salt tolerance of the *antiVcHKT1;1*$^{DK}$ mutant was intermediate between those of SH and DK (Fig. 1), indicating that although *VcHKT1;1* plays a significant role in promoting $Na^+$ exclusion from roots to leaves and enhancing salt tolerance in blueberry, other key genes are also involved in this process. We thus conducted WGCNA focusing on the DEGs between SH and DK. The hub genes encoding ion transport proteins, such as *VcHAK5*, *VcNHX1*, and *VcNHX2*, were identified in high-correlation modules (Figs. 2–4).

*VcHAK5* encodes a high-affinity $K^+$ transporter that belongs to the HAK family, with the highest homology to AtHAK5 (Fig. 4). Members of the HAK family are involved in mediating $K^+$ fluxes, $Na^+$ transport, and $Na^+/K^+$ homeostasis (Shen *et al.* 2015; Zhu 2016; Zhang *et al.* 2019; Wang *et al.* 2020, 2024). For instance, in *Arabidopsis*, ethylene signaling increases the transcription level of *AtHAK5*, promoting $K^+$ homeostasis and enhancing salt tolerance (Kim *et al.* 2012). Based on our findings, VcHAK5 was located in the plasma membrane and showed $K^+$ transport activity but not $Na^+$ transport activity in yeast (Fig. 6-A, C and D). The *VcHAK5* knockdown mutants exhibited hypersensitivity to salt stress and an increased $Na^+/K^+$ ratio (Fig. 7), suggesting that *VcHAK5* probably regulates $K^+$ content and contributes to maintaining $Na^+/K^+$ homeostasis, thereby promoting blueberry salt tolerance. This finding aligns with studies in tomatoes, where SlHAK20 regulates the $Na^+/K^+$ ratio in roots by mediating the transport of $Na^+$ and $K^+$, and knockout mutations in SlHAK20 lead to hypersensitivity to salt stress (Wang *et al.* 2020). Notably, rice OsHAK5 plays a role in regulating the transport of $K^+$ from roots to shoots, while maize ZmHAK5 mainly regulates $K^+$ absorption under low potassium stress (Yang *et al.* 2014; Qin *et al.* 2019). Some members of the HAK family are involved in physiological processes beyond root $K^+$ uptake, including $K^+$ efflux at the roots or guard cells, long-distance $K^+$ transport, and $K^+$ uptake in pollen (Osakabe *et al.* 2013; Han *et al.* 2016; Nieves-Cordones *et al.* 2020). These suggest that the functions and roles of HAK5 are diverse across different plant species. However, the transcriptional regulation of *HAK5* has been less extensively studied. We therefore analyzed the promoter region of *VcHAK5*, and identified multiple *cis*-regulatory elements associated with environmental stress and hormonal signaling, including

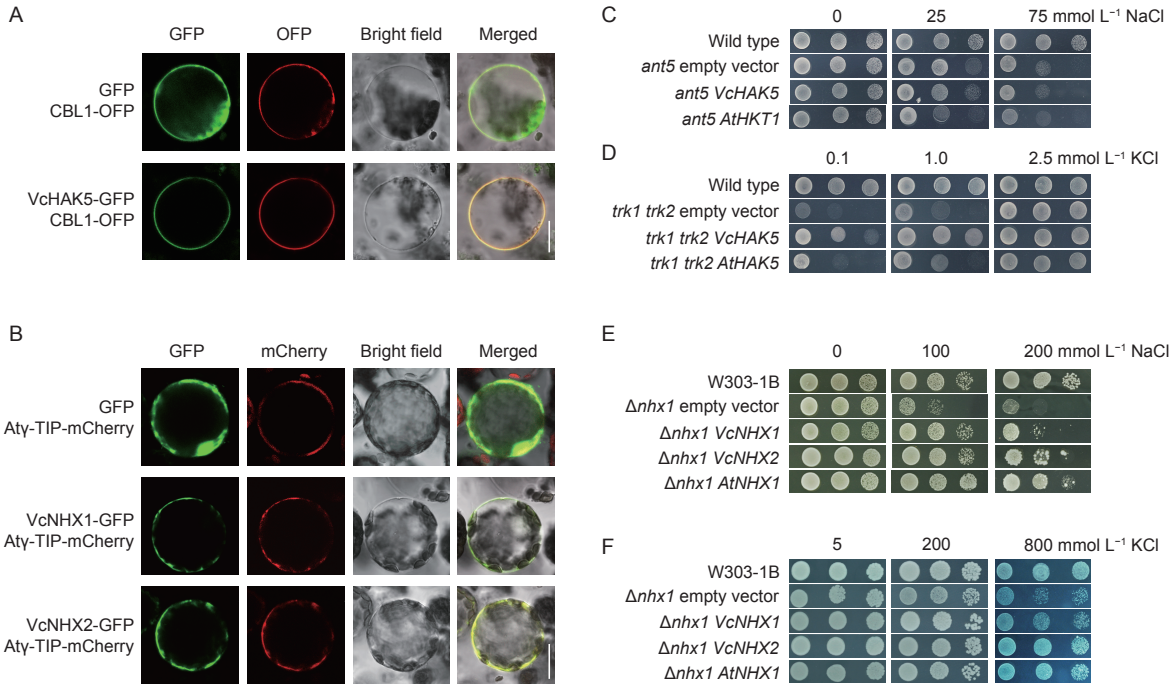



**Fig. 6 Function characterization of VcHAK5, VcNHX1, and VcNHX2.** A and B, subcellular localization of the VcHAK5, VcNHX1, and VcNHX2 proteins. Images in *Nicotiana benthamiana* protoplasts co-expressing VcHAK5-GFP and AtCBL1-OFP (a plasma membrane-localized marker) (A), and VcNHX1-GFP and VcNHX2-GFP with Atγ-TIP-mCherry (the tonoplast localized marker) (B). The vector with GFP was a positive control. Similar results with three independent experiments. Bar=20 μm. C and D, VcHAK5 function as a $K^+$-selective transporter in yeast. VcHAK5 and AtHKT1 were expressed in the yeast strain *ant5* grown on the medium containing 1 mmol $L^{-1}$ KCl and varying NaCl concentrations (C). VcHAK5 and AtHKT1 were expressed in the yeast strain *trk1 trk2* grown on a medium with indicated KCl concentrations (D). The wild-type strain and empty vector mutants were used as the negative controls. *ant5* with *AtHKT1* and *trk1 trk2* with the *AtHAK5* were positive controls. E and F, VcNHX1 and VcNHX2 function as $Na^+$ and $K^+$ transporters in yeast complementation. Expressing the indicated genes rescued growth inhibition in Δ*nhx1* yeast at high $Na^+$ (E) and $K^+$ (F) concentrations. The mutant Δ*nhx1* with *AtNHX1* and W303-1B served as controls. Similar results were obtained in five independent experiments.

abscisic acid-responsive elements (ABREs) and MYB-binding motifs (Appendix M). ABREs are key components of ABA-mediated stress signaling pathways, especially under drought and salinity conditions, while MYB-binding sites are commonly involved in transcriptional responses to osmotic stress and secondary metabolism (Chen *et al.* 2019). The presence of these elements suggests that the root-specific induction of *VcHAK5* may be regulated by stress-responsive transcription factors and/or hormone signaling cascades, enabling plants to fine-tune potassium uptake under adverse environmental conditions. These findings provide a basis for further functional studies on the transcriptional control of VcHAK5 and its role in stress adaptation.

*VcNHX1* and *VcNHX2* encode NHX-type cation/$H^+$ transporters (Fig. 4), which are involved in $Na^+(K^+)/H^+$ exchange, contributing to $K^+$ homeostasis and salt tolerance. In *Arabidopsis*, the NHX7 and NHX8 (with NHX7 also known as SOS1) have been shown to facilitate $Na^+$ efflux from the roots (Zhu 2016; Yang and Guo 2018). AtNHX1–AtNHX4 are located in the tonoplast, while AtNHX5 and AtNHX6 are located in endosomes, which are important for regulating vacuolar and vesicular pH, as well as $Na^+$ and $K^+$ homeostasis (Bassil *et al.* 2011). Tomatoes *LeNHX2* is abundantly expressed in roots and stems and enhances salt tolerance under high external $K^+$ conditions (Rodríguez-Rosales *et al.* 2008). *HtNHX1* and *HtNHX2* from *Jerusalem artichoke* were upregulated in the roots and stems in response to increasing salinity levels, and the expression of *HtNHX2* in rice enhanced salt tolerance (Zeng *et al.* 2018). Here, we showed that *VcNHX1* and *VcNHX2* encoded the $Na^+$- and $K^+$- transporter localized to the tonoplast (Fig. 6-B, E and F). Additionally, the knockdown mutants of *VcNHX1* and *VcNHX2* displayed a higher $Na^+/K^+$ ratio and greater sensitivity to salt stress (Fig. 7), indicating that *VcNHX1* and *VcNHX2* may regulate blueberry salt tolerance by maintaining $Na^+/K^+$ homeostasis. It is worth noting that the earliest studies in *Arabidopsis* suggested that AtNHX1 functions as a $Na^+/H^+$ exchanger, compartmentalizing $Na^+$ into vacuoles to promote plant salt tolerance (Apse *et al.* 2003). However, subsequent research found that AtNHX1 and AtNHX2 act as $K^+/H^+$ exchangers, playing a role in maintaining cytosolic $K^+$ concentration and pH under salt stress conditions (Barragán *et al.* 2012). Recent studies have also indicated that wheat TaNHX2 functions as a $K^+/H^+$ exchanger (Li *et al.* 2024). Additionally, the promoter regions of *VcNHX1* and *VcNHX2* contain several *cis*-regulatory elements associated with hormonal regulation and stress responses (Appendix M). Therefore, the molecular mechanism of VcNHX1 and VcNHX2 and their roles in responding to salt stress still require further investigation.

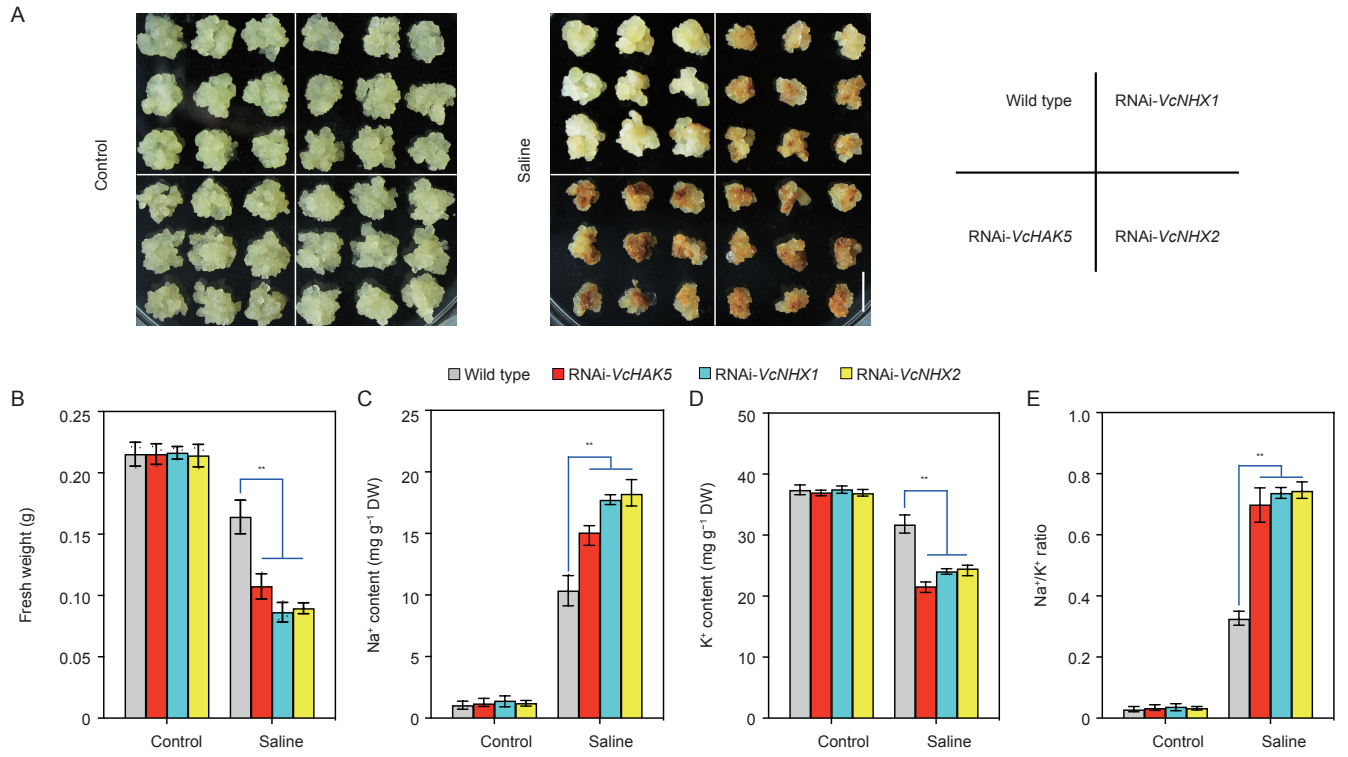



**Fig. 7 Knockdown of *VcHAK5*, *VcNHX1*, and *VcNHX2* decreases salt tolerance in blueberry.** A, phenotypes of wild-type and *RNAi-VcHAK5*, *RNAi-VcNHX1*, and *RNAi-VcNHX2* blueberry calli under NaCl treatment and control conditions. Photographs show 20-d-old blueberry calli grown on WPM medium with 150 mmol $L^{-1}$ NaCl for 5 d. Bar=0.5 cm. Similar results were observed in three independent experiments. B–E, fresh weight (B), $Na^+$ (C), and $K^+$ (D) contents, and $Na^+/K^+$ ratios of blueberry calli under 150 mmol $L^{-1}$ NaCl treatment. Data in B–E are presented as means±SD from three independent experiments, with statistical analysis conducted using two-way ANOVA in different samples. Significant differences are indicated as: $^{**}$, $P$<0.01.

Numerous studies have demonstrated that $Na^+$ and $K^+$ transporters are primarily expressed in the roots, where they play a key role in regulating $Na^+$ and $K^+$ in the leaves (Cao *et al.* 2019; Huang *et al.* 2020; Zhang *et al.* 2023), suggesting that the root tissue determinants of $Na^+/K^+$ ratios are important for improving salt tolerance in crops. For example, the $Na^+/H^+$ antiporter SOS1 facilitates root $Na^+$ efflux, thereby decreasing cytosolic $Na^+$ accumulation and reducing toxicity (Shi *et al.* 2002). The $Na^+$-preferential transporters like HKT1, ZmHAK4, and OsHAK12 facilitate $Na^+$ unloading in the root xylem, preventing excessive $Na^+$ accumulation in leaves (Byrt *et al.* 2014; Cao *et al.* 2019; Huang *et al.* 2020; Zhang *et al.* 2021). The $K^+$-selective transporter ZmHAK5 is primarily expressed in roots and regulates $K^+$ uptake and $K^+$ distribution (Qin *et al.* 2019). In our study, we found that *VcNHX1*, *VcNHX2*, *VcHAK5*, and *VcHKT1;1* were significantly upregulated in the roots of the salt-tolerant blueberry cultivar DK under salt stress (Figs. 4, 5 and 9), indicating that the high expression of ion ($Na^+$ and $K^+$) transporter genes in the roots is associated with salt tolerance in blueberry. To further verify this hypothesis, we conducted grafting experiments. The reciprocal grafting of SH/DK (with DK as the rootstock and SH as the scion) reduced $Na^+$ content and $Na^+/K^+$ ratio in the leaves, thereby improving salt tolerance. In contrast, DK/SH (with SH as the rootstock and DK as the scion) exhibited greater sensitivity to salt stress (Fig. 7). This result is consistent with findings in cucumber, pumpkin, and tomato. Reciprocal grafting experiments in cucumber and pumpkin demonstrated that pumpkin rootstocks have a higher capacity for $Na^+$ exclusion and retention, and enhanced salt tolerance in cucumber (Davoudi *et al.* 2022). In tomatoes, the variations in fruit yield among different graft combinations were primarily linsed to the rootstocks' abilities to regulate saline ion transport. A strong negative correlation was observed between fruit yield and leaf $Na^+$ or $Cl^-$ concentrations under salt conditions (Estañ *et al.* 2005). These results suggest that employing salt-tolerant rootstocks for grafting is an effective strategy to enhance salt tolerance in blueberries. In future research, salt tolerance in rootstocks could be improved through molecular breeding, combined with grafting techniques to effectively shorten the breeding cycle and reduce the cost of developing salt-tolerant blueberry cultivars.

In summary, our transcriptome sequencing and knockdown mutation analysis indicate that *VcHAK5*, *VcNHX1*, and *VcNHX2* are critical for salt tolerance in blueberry. *VcHAK5* encodes a $K^+$-selective transporter, while *VcNHX1* and *VcNHX2* encode $Na^+/H^+$ and $K^+/H^+$ antiporters, all of which were upregulated in the roots of the salt-tolerant cultivar DK under salt stress (Fig. 9). Grafting blueberry onto DK rootstocks improved salt tolerance by reducing leaf $Na^+$ content, lowering the $Na^+/K^+$ ratio, and mitigating photosynthetic damage. This study provides the first comprehensive exploration of the molecular mechanisms underlying blueberries' response to salt

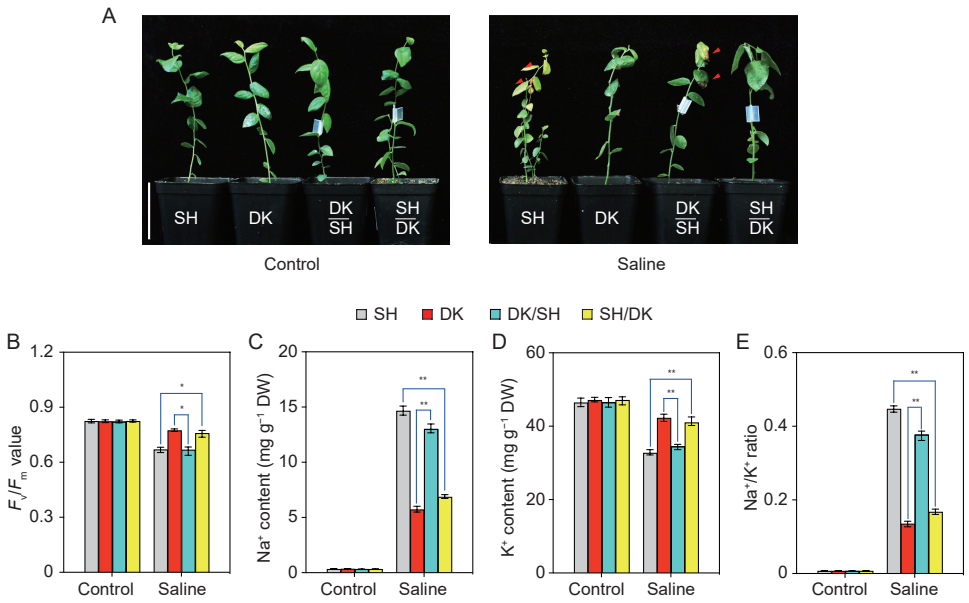



**Fig. 8 Reciprocal grafting of 'Sweetheart' (SH) and 'Duke' (DK) showing differing salt sensitivity.** A, phenotypes of the reciprocal grafting of SH and DK under salt treatment and control. Rootstocks and scions were derived from one-year-old blueberry seedlings. The grafted seedlings were cultured for 30 d and then treated with 200 mmol $L^{-1}$ NaCl for 3 d. DK/SH denotes SH as the rootstock and DK as the scion, and *vice versa* for SH/DK. Scale bar=7 cm. Similar results with three independent experiments. B, $F_v/F_m$ values. C–E, The $Na^+$ content (C), $K^+$ content (D), and $Na^+/K^+$ ratio (E) were measured in SH, DK, DK/SH, and SH/DK under salt treatment compared to the control. DW represents dry weight. Data in B–E are means±SD from three replicates. The color scheme is consistent across subpanel B–E. Statistical significance was assessed using two-way ANOVA: *, $P<0.05$; **, $P<0.01$.

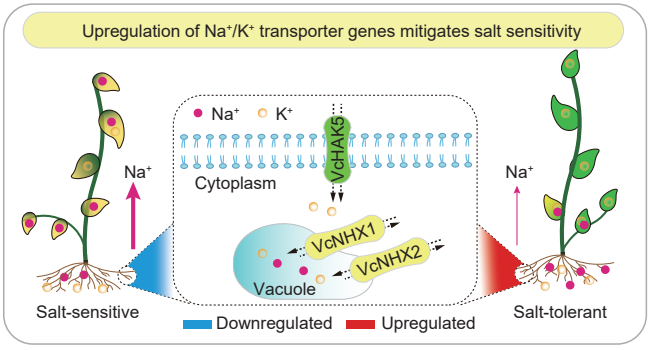



**Fig. 9 Root upregulation of $Na^+/K^+$ transporter genes *VcHAK5*, *VcNHX1*, and *VcNHX2* mitigates salt sensitivity in blueberry.** Under salt stress, the salt-tolerant cultivar 'Duke' exhibited strong upregulation of *VcHAK5*, *VcNHX1*, and *VcNHX2* in roots, accompanied by lower leaf $Na^+$ accumulation compared to the salt-sensitive cultivar 'Sweetheart', which showed weaker gene expression and higher leaf $Na^+$ content. *VcHAK5* encodes a $K^+$ transporter localized to the plasma membrane, whereas *VcNHX1* and *VcNHX2* encode $Na^+/K^+$ transporters localized to the vacuolar membrane. Upregulation of these transporters contributes to maintaining $Na^+/K^+$ homeostasis and enhancing salt tolerance in blueberries.

stress. It suggests that variations in $Na^+$ and $K^+$ transporters associated with grafting techniques play a crucial role in $Na^+/K^+$ homeostasis and salt tolerance in fruit trees. These findings offer valuable insights for molecular and traditional breeding aimed at enhancing salt tolerance in cultivated blueberry and other fruit crops.

## 5. Conclusion

Our findings revealed that *VcHAK5*, *VcNHX1*, and *VcNHX2* are key regulators of salt tolerance in blueberry, and that salt-resistant roots reduce $Na^+$ accumulation and maintain $Na^+/K^+$ homeostasis under salt stress (Fig. 9). Thus, our research provides novel evidence that ion transporter regulation in roots is a crucial determinant of salt tolerance in cultivated blueberry.

## Acknowledgements

This work was supported by the Key Research and Development Plan of Shandong Province, China (2024LZGCQY025), the National Natural Science Foundation of China (32101555), and the 5·5 Engineering Research & Innovation Team Project of Beijing Forestry University (BLRC2023B08). We thank Prof. Caifu Jiang from China Agricultural University for stimulating discussions, Prof. Yadong Li from Jilin Agricultural University for providing the blueberry cultivars, Prof. Zhaorong Hu from China Agricultural University for supplying the W303-1B and Δ*nhx1* yeast strains, and Prof. Yuanyuan Li from Shandong Agricultural University, China for supplying the vector pRI-RNAi.

## Declaration of competing interest

The authors declare that they have no conflict interest.

## Declaration of generative AI and AI-assisted technologies in the writing process

The authors declare that they did not use AI in the preparation

and writing of this manuscript.

**Appendices** associated with this paper are available at https://doi.org/10.1016/j.jia.2025.12.004

## References


Apse M P, Aharon G S, Snedden W A, Blumwald E. 1999. Salt tolerance conferred by overexpression of a vacuolar $Na^+/H^+$ antiport in *Arabidopsis*. *Science*, **285**, 1256–1258.

Apse M P, Sottosanto J B, Blumwald E. 2003. Vacuolar cation/$H^+$ exchange, ion homeostasis, and leaf development are altered in a T-DNA insertional mutant of *AtNHX1*, the *Arabidopsis* vacuolar $Na^+/H^+$ antiporter. *The Plant Journal*, **36**, 229–239.

Barragán V, Leidi E O, Andrés Z, Rubio L, De Luca A, Fernández J A, Cubero B, Pardo J M. 2012. Ion exchangers NHX1 and NHX2 mediate active potassium uptake into vacuoles to regulate cell turgor and stomatal function in *Arabidopsis*. *The Plant Cell*, **24**, 1127–1142.

Bassil E, Ohto M A, Esumi T, Tajima H, Zhu Z, Cagnac O, Belmonte M, Peleg Z, Yamaguchi T, Blumwald E. 2011. The *Arabidopsis* intracellular $Na^+/H^+$ antiporters NHX5 and NHX6 are endosome associated and necessary for plant growth and development. *Plant Cell*, **23**, 224–239.

Batistic O, Sorek N, Schültke S, Yalovsky S, Kudla J. 2008. Dual fatty acyl modification determines the localization and plasma membrane targeting of CBL/CIPK $Ca^{2+}$ signaling complexes in *Arabidopsis*. *The Plant Cell*, **20**, 1346–1362.

Blumwald E, Poole R J. 1985. $Na^+/H^+$ antiport in isolated tonoplast vesicles from storage tissue of *Beta vulgaris*. *Plant Physiology*, **78**, 163–167.

Bryla D R, Scagel C F, Lukas S B, Sullivan D M. 2021. Ion-specific limitations of sodium chloride and calcium chloride on growth, nutrient uptake, and mycorrhizal colonization in northern and southern highbush blueberry. *Journal of the American Society for Horticultural Science*, **146**, 399–410.

Byrt C S, Xu B, Krishnan M, Lightfoot D J, Athman A, Jacobs A K, Watson-Haigh N S, Plett D, Munns R, Tester M, Gilliham M. 2014. The $Na^+$ transporter, TaHKT1;5d, limits shoot $Na^+$ accumulation in bread wheat. *Plant Journal*, **80**, 516–526.

Calero F, Gómez N, Ariño J, Ramos J. 2000. Trk1 and trk2 define the major $K^+$ transport system in fission yeast. *Journal of Bacteriology*, **182**, 394–399.

Cao Y B, Liang X Y, Yin P, Zhang M, Jiang C F. 2019. A domestication-associated reduction in $K^+$-preferring HKT transporter activity underlies maize shoot $K^+$ accumulation and salt tolerance. *New Phytologist*, **222**, 301–317.

Chen G, Hu Q, Luo L, Yang T, Zhang S, Hu Y, Yu L, Xu G. 2015. Rice potassium transporter OsHAK1 is essential for maintaining potassium-mediated growth and functions in salt tolerance over low and high potassium concentration ranges. *Plant, Cell & Environment*, **38**, 2747–2765.

Chen H, Chen X, Gu H, Wu B, Zhang H, Yuan X, Cui X. 2014. *Gmhkt1;4*, a novel soybean gene regulating $Na^+/K^+$ ratio in roots enhances salt tolerance in transgenic plants. *Plant Growth Regulation*, **73**, 299–308.

Chen K Q, Song M R, Guo Y N, Liu L F, Xue H, Dai H Y, Zhang Z H. 2019. *Mdmyb46* could enhance salt and osmotic stress tolerance in apple by directly activating stress-responsive signals. *Plant Biotechnology Journal*, **17**, 2341–2355.

Chen W R, Shao J Y, Ye M J, Yu K D, Bednarek S Y, Duan X, Guo W. 2017. Blueberry VcLON2, a peroxisomal ion protease, is involved in abiotic stress tolerance. *Environmental and Experimental Botany*, **134**, 1–11.

Coba de la Peña T, Redondo F J, Manrique E, Lucas M M, Pueyo J J. 2010. Nitrogen fixation persists under conditions of salt stress in transgenic *Medicago truncatula* plants expressing a cyanobacterial flavodoxin. *Plant Biotechnology Journal*, **8**, 954–965.

Colle M, Leisner C P, Wai C M, Ou S, Bird K A, Wang J, Wisecaver J H, Yocca A E, Alger E I, Tang H, Xiong Z, Callow P, Ben-Zvi G, Brodt A, Baruch K, Swale T, Shiue L, Song G Q, Childs K L, Schilmiller A, *et al.* 2019. Haplotype-phased genome and evolution of phytonutrient pathways of tetraploid blueberry. *GigaScience*, **8**, 1–15.

Davenport R J, Munoz-Mayor A, Jha D, Essah P A, Rus A, Tester M. 2007. The $Na^+$ transporter AtHKT1;1 controls retrieval of $Na^+$ from the xylem in *Arabidopsis*. *Plant Cell and Environment*, **30**, 497–507.

Davoudi M, Song M, Zhang M, Chen J, Lou Q. 2022. Long-distance control of pumpkin rootstock over cucumber scion under drought stress as revealed by transcriptome sequencing and mobile mRNAs identifications. *Horticulture Research*, **9**, uhab033.

Deinlein U, Stephan A B, Horie T, Luo W, Xu G H, Schroeder J I. 2014. Plant salt-tolerance mechanisms. *Trends in Plant Science*, **19**, 371–379.

Estañ M T, Martinez-Rodriguez M M, Perez-Alfocea F, Flowers T J, Bolarin M C. 2005. Grafting raises the salt tolerance of tomato through limiting the transport of sodium and chloride to the shoot. *Journal of Experimental Botany*, **56**, 703–712.

Gaxiola R A, Rao R, Sherman A, Grisafi P, Alper S L, Fink G R. 1999. The *Arabidopsis thaliana* proton transporters, AtNHX1 and AVP1, can function in cation detoxification in yeast. *Proceedings of the National Academy of Sciences of the United States of America*, **96**, 1480–1485.

Han M, Wu W, Wu W H, Wang Y. 2016. Potassium transporter KUP7 is involved in $K^+$ acquisition and translocation in *Arabidopsis* root under $K^+$-limited conditions. *Molecular Plant*, **9**, 437–446.

Henderson S W, Dunlevy J D, Wu Y, Blackmore D H, Walker R R, Edwards E J, Gilliham M, Walker A R. 2018. Functional differences in transport properties of natural HKT1;1 variants influence shoot $Na^+$ exclusion in grapevine rootstocks. *New Phytologist*, **217**, 1113–1127.

Huang L, Kuang L, Wu L, Shen Q, Han Y, Jiang L, Wu D, Zhang G. 2020. The HKT transporter HvHKT1;5 negatively regulates salt tolerance. *Plant Physiology*, **182**, 584–596.

Ishikawa T, Shabala S. 2019. Control of xylem $Na^+$ loading and transport to the shoot in rice and barley as a determinant of differential salinity stress tolerance. *Physiologia Plantarum*, **165**, 619–631.

Kalt W, Cassidy A, Howard L R, Krikorian R, Stull A J, Tremblay F, Zamora-Ros R. 2020. Recent research on the health benefits of blueberries and their anthocyanins. *Advances in Nutrition*, **11**, 224–236.

Kaundal A, Sandhu D, Duenas M, Ferreira J F S. 2019. Expression of the high-affinity $K^+$ transporter 1 (*PpHKT1*) gene from almond rootstock 'nemaguard' improved salt tolerance of transgenic *Arabidopsis*. *PLoS ONE*, **14**, e0214473.

Kim M J, Ruzicka D, Shin R, Schachtman D P. 2012. The *Arabidopsis* AP2/ERF transcription factor *RAP2.11* modulates plant response to low-potassium conditions. *Molecular Plant*, **5**, 1042–1057.

Li H, Yu M, Du X Q, Wang Z F, Wu W H, Quintero F J, Jin X H, Li H D, Wang Y. 2017. NRT1.5/NFP7.3 functions as a proton-coupled $H^+/K^+$ antiporter for $K^+$ loading into the xylem in *Arabidopsis*. *Plant Cell*, **29**, 2016–2026.

Li J P, Liu X B, Chang S M, Chu W, Lin J, Zhou H, Hu Z, Zhang M, Xin M, Yao Y, Guo W, Xie X, Peng H, Ni Z, Sun Q, Long Y, Hu Z. 2024. The potassium transporter TaNHX2 interacts with TaGAD1 to promote drought tolerance via modulating stomatal aperture in wheat. *Science Advances*, **10**, eadk4027.

Liang Y F, Bai J Y, Xie Z L, Lian Z Y, Guo J, Zhao F Y, Liang Y, Huo H Q, Gong H J. 2023. Tomato sucrose transporter SlSUT4 participates in flowering regulation by modulating gibberellin biosynthesis. *Plant Physiology*, **192**, 1080–1098.

Martínez-Cordero M A, Martínez V, Rubio F. 2004. Cloning and functional characterization of the high-affinity $K^+$ transporter HAK1 of pepper. *Plant Molecular Biology*, **56**, 413–421.

Mäser P, Thomine S, Schroeder J I, Ward J M, Hirschi K, Sze H, Talke I N, Amtmann A, Maathuis F J, Sanders D, Harper J F, Tchieu J, Gribskov M, Persans M W, Salt D E, Kim S A, Guerinot M L. 2001. Phylogenetic relationships within cation transporter families of *Arabidopsis*. *Plant Physiology*, **126**, 1646–1667.

Munns R, James R A, Xu B, Athman A, Conn S J, Jordans C, Byrt C S, Hare R A, Tyerman S D, Tester M, Plett D, Gilliham M. 2012. Wheat grain yield on saline soils is improved by an ancestral $Na^+$ transporter gene. *Nature Biotechnology*, **30**, 360–364.

Munns R, Tester M. 2008. Mechanisms of salinity tolerance. *Annual Review of Plant Biology*, **59**, 651–681.

Muralitharan M S, Van Steveninck R F M, Chandler S E. 1990. Growth characteristics and ion contents of non-selected and salt-selected callus lines of highbush blueberry (*Vaccinium corymbosum*) cultivars Bluecrop and Denise blue. *Plant Cell Reports*, **9**, 151–155.

Nieves-Cordones M, Lara A, Silva M, Amo J, Rodriguez-Sepulveda P, Rivero R M, Martínez V, Botella M A, Rubio F. 2020. Root high-affinity $K^+$ and $Cs^+$ uptake and plant fertility in tomato plants are dependent on the activity of the high-affinity $K^+$ transporter SlHAK5. *Plant Cell and Environment*, **43**, 1707–1721.

Osakabe Y, Arinaga N, Umezawa T, Katsura S, Nagamachi K, Tanaka H, Ohiraki H, Yamada K, Seo S U, Abo M, Yoshimura E, Shinozaki K, Yamaguchi-Shinozaki K. 2013. Osmotic stress responses and plant growth controlled by potassium transporters in *Arabidopsis*. *The Plant Cell*, **25**, 609–624.

Qin X J, Hu J, Xu G, Song H F, Zhang L Y, Cao Y B. 2023. An efficient transformation system for fast production of VcCHS transgenic blueberry callus and its expressional analysis. *Plants* (Basel), **12**, 2905.

Qin Y J, Wu W H, Wang Y. 2019. ZmHAK5 and ZmHAK1 function in $K^+$ uptake and distribution in maize under low $K^+$ conditions. *Journal of Integrative Plant Biology*, **61**, 691–705.

Qu D H, Wu F L, Zhao X H, Zhu D, Gu L, Yang L, Zhao W, Sun Y, Yang J, Tian W, Su H, Wang L. 2022. A bzip transcription factor *Vabzip12* from blueberry induced by dark septate endocyte improving the salt tolerance of transgenic *Arabidopsis*. *Plant Science*, **315**, 111135.

Quintero F J, Ohta M, Shi H, Zhu J K, Pardo J M. 2002. Reconstitution in yeast of the *Arabidopsis* SOS signaling pathway for $Na^+$ homeostasis. *Proceedings of the National Academy of Sciences of the United States of America*, **99**, 9061–9066.

Ren Z H, Gao J P, Li L G, Cai X L, Huang W, Chao D Y, Zhu M Z, Wang Z Y, Luan S, Lin H X. 2005. A rice quantitative trait locus for salt tolerance encodes a sodium transporter. *Nature Genetics*, **37**, 1141–1146.

Ródenas R, Ragel P, Nieves-Cordones M, Martínez-Martínez A, Amo J, Lara A, Martínez V, Quintero F J, Pardo J M, Rubio F. 2021. Insights into the mechanisms of transport and regulation of the *Arabidopsis* high-affinity $K^+$ transporter HAK51. *Plant Physiology*, **185**, 1860–1874.

Rodríguez-Rosales M P, Jiang X Y, Gálvez F J, Aranda M N, Cubero B, Venema K. 2008. Overexpression of the tomato $K^+/H^+$ antiporter LeNHX2 confers salt tolerance by improving potassium compartmentalization. *New Phytologist*, **179**, 366–377.

Rubio F, Gassmann W, Schroeder J I. 1995. Sodium-driven potassium uptake by the plant potassium transporter HKT1 and mutations conferring salt tolerance. *Science*, **270**, 1660–1663.

Schachtman D P, Schroeder J I. 1994. Structure and transport mechanism of a high-affinity potassium uptake transporter from higher plants. *Nature*, **370**, 655–658.

Shen Y, Shen L, Shen Z, Jing W, Ge H, Zhao J, Zhang W. 2015. The potassium transporter OsHAK21 functions in the maintenance of ion homeostasis and tolerance to salt stress in rice. *Plant Cell Environment*, **38**, 2766–2779.

Shi H, Quintero F J, Pardo J M, Zhu J K. 2002. The putative plasma membrane $Na^+/H^+$ antiporter SOS1 controls long-distance $Na^+$ transport in plants. *The Plant Cell*, **14**, 465–477.

Song G Q, Sink K C, Walworth A E, Cook M A, Allison R F, Lang G A. 2013. Engineering cherry rootstocks with resistance to Prunus necrotic ring spot virus through RNAi-mediated silencing. *Plant Biotechnology Journal*, **11**, 702–708.

Song H F, Cao Y B, Zhao X Y, Zhang L Y. 2023. $Na^+$-preferential ion transporter HKT1;1 mediates salt tolerance in blueberry. *Plant Physiology*, **194**, 511–529.

Vashisth T, Johnson L K, Malladi A. 2011. An efficient RNA isolation procedure and identification of reference genes for normalization of gene expression in blueberry. *Plant Cell Reports*, **30**, 2167–2176.

Venema K, Quintero F J, Pardo J M, Donaire J P. 2002. The *Arabidopsis* $Na^+/H^+$ exchanger AtNHX1 catalyzes low-affinity $Na^+$ and $K^+$ transport in reconstituted liposomes. *Journal of Biological Chemistry*, **277**, 2413–2418.

Wang A B, Wang L, Liu K, Liang K H, Yang S W, Cao Y B, Zhang L Y. 2022. Comparative transcriptome profiling reveals the defense pathways and mechanisms in the leaves and roots of blueberry to drought stress. *Fruit Research*, **2**, 1–15.

Wang L M, Wang Y Y, Yin P, Jiang C F, Zhang M. 2024. ZmHAK17 encodes a $Na^+$-selective transporter that promotes maize seed germination under salt conditions. *New Crops*, **1**, 100024.

Wang Z, Hong Y, Zhu G, Li Y, Niu Q, Yao J, Hua K, Bai J, Zhu Y, Shi H, Huang S, Zhu J K. 2020. Loss of salt tolerance during tomato domestication conferred by variation in a $Na^+/K^+$ transporter. *The EMBO Journal*, **39**, e103256.

Xu H, Zou Q, Yang G, Jiang S, Fang H, Wang Y, Zhang J, Zhang Z, Wang N, Chen X. 2020. *Mdmyb6* regulates anthocyanin formation in apple both through direct inhibition of the biosynthesis pathway and through substrate removal. *Horticulture Research*, **7**, 72.

Yang L, Li M, Shen M, Bu S, Zhu B, He F, Zhang X, Gao X, Xiao J. 2022. Chromosome-level genome assembly and annotation of the native Chinese wild blueberry *Vaccinium bracteatum*. *Fruit Research*, **2**, 1–14.

Yang T, Zhang S, Hu Y, Wu F, Hu Q, Chen G, Cai J, Wu T, Moran N, Yu L, Xu G. 2014. The role of a potassium transporter OsHAK5 in potassium acquisition and transport from roots to shoots in rice at low potassium supply levels. *Plant Physiology*, **166**, 945–959.

Yang Y Q, Guo Y. 2018. Elucidating the molecular mechanisms mediating plant salt-stress responses. *New Phytologist*, **217**, 523–539.

Yokoi S, Quintero F J, Cubero B, Ruiz M T, Bressan R A, Hasegawa P M, Pardo J M. 2002. Differential expression and function of *Arabidopsis thaliana* NHX $Na^+/H^+$ antiporters in the salt stress response. *Plant Journal*, **30**, 529–539.

van Zelm E, Zhang Y X, Testerink C. 2020. Salt tolerance mechanisms of plants. *Annual Review of Plant Biology*, **71**, 403–433.

Zeng Y, Li Q, Wang H, Zhang J, Du J, Feng H, Blumwald E, Yu L, Xu G. 2018. Two NHX-type transporters from *Helianthus tuberosus* improve the tolerance of rice to salinity and nutrient deficiency stress. *Plant Biotechnology Journal*, **16**, 310–321.

Zhang L, Sun X, Li Y, Luo X, Song S, Chen Y, Wang X, Mao D, Chen L, Luan S. 2021. Rice $Na^+$-permeable transporter OsHAK12 mediates shoots $Na^+$ exclusion in response to salt stress. *Frontiers Plant Science*, **12**, 771746.

Zhang M, Cao Y B, Wang Z, Wang Z Q, Shi J, Liang X, Song W, Chen Q, Lai J, Jiang C F. 2018. A retrotransposon in an HKT1 family sodium transporter causes variation of leaf $Na^+$ exclusion and salt tolerance in maize. *New Phytologist*, **217**, 1161–1176.

Zhang M, Li Y, Liang X, Lu M, Lai J, Song W, Jiang C F. 2023. A teosinte-derived allele of an HKT1 family sodium transporter improves salt tolerance in maize. *Plant Biotechnology Journal*, **21**, 97–108.

Zhang M, Liang X Y, Wang L M, Cao Y B, Song W B, Shi J P, Lai J S, Jiang C F. 2019. A HAK family $Na^+$ transporter confers natural variation of salt tolerance in maize. *Nature Plants*, **5**, 1297–1308.

Zhao C, Zhang H, Song C, Zhu J K, Shabala S. 2020. Mechanisms of plant responses and adaptation to soil salinity. *Innovation* (Camb), **1**, 100017.

Zhong H, Liu Z, Zhang F, Zhou X, Sun X, Li Y, Liu W, Xiao H, Wang N, Lu H, Pan M, Wu X, Zhou Y. 2022. Metabolomic and transcriptomic analyses reveal the effects of self- and hetero-grafting on anthocyanin biosynthesis in grapevine. *Horticulture Research*, **9**, uhac103.

Zhong J J, Gu J J, Guo Y P, You S, Liao F, Chen W, Guo W. 2019. Blueberry VcLON1 protease increases iron use efficiency by alleviating chloroplast oxidative stress. *Plant and Soil*, **445**, 533–548.

Zhu J K. 2016. Abiotic stress signaling and responses in plants. *Cell*, **167**, 313–324.

Executive Editor-in-Chief Sanwen Huang
Managing Editor Lingyun Weng